Spacetime structures in simple quantum systems

1997 J. Phys. A: Math. Gen. 30 L277

(http://iopscience.iop.org/0305-4470/30/9/004)

J. Phys. A: Math. Gen. **30** (1997) L277–L283. Printed in the UK PII: S0305-4470(97)81100-6

LETTER TO THE EDITOR

Spacetime structures in simple quantum systems

Frank Großmann†, Jan-Michael Rost† and Wolfgang P Schleich‡

† Albert-Ludwigs-Universität, Fakultät für Physik, Hermann-Herder-Strasse 3, D-79104, Freiburg, Germany

‡ Abteilung für Quantenphysik, Universität Ulm, D-89069 Ulm, Germany

Received 20 January 1997

Abstract. Recently W Kinzel [1995 *Phys. Bl.* **51** 1190] has argued that even simple quantum systems can exhibit surprising phenomena. As an example he presented the formation of canals and ridges in the time-dependent probability density of a particle caught in a square well with infinitely high walls. We show how these structures emerge from the wavefunction and present a simple derivation of their location in the spacetime continuum.

Prominent structures in the probability density of quantum states have attracted much attention. They are known as *scars* for time-independent problems where certain eigenstates have regions of high amplitude along periodic orbits of the classical dynamics for the same system [1]. This phenomenon has helped us to understand the links between classical and quantum mechanics in more detail [2]. In the time domain the reconstruction or partial reconstruction of the initial spatial probability distribution is known as *revivals* and has played an important role in the understanding of wavepacket dynamics [3]. The combination of spatial and temporal structures in a probability density has only recently entered the focus of attention. Kinzel [4] has numerically studied the time evolution of a particle in an infinitely-high potential well. He used a Gaussian initial wavepacket centred close to the left wall and furnished with a momentum pointing towards the right. In a three-dimensional plot of the absolute square of the wavefunction over position and time, regular structures in the shape of valleys and hills appear. Clearly, such structures must be an interference phenomenon. However, their origin is not as obvious as one might expect for such a simple system and has not been given in [4]. Berry and Klein have found similar patterns in the Talbot effect and Berry has also studied fractal probability densities in the spacetime continuum for multi-dimensional box potentials [5]. In the latter case he has used a special initial state with equal probability amplitude at each point in the box. Stifter *et al* [6], using Gaussian initial wavefunctions, have shown that the structures in the probability distribution can be viewed as a consequence of the interference term in the Wigner function. In this letter we will use an initial state which is composed of the first N eigenfunctions with equal weights. This allows us to study the emerging pattern in spacetime as a function of N. It will turn out that the structures in the amplitude distribution arise from a cancellation of terms in the wavefunction and that the parameter N controls the resolution of the pattern. Our analysis borrows a mathematical technique which is familiar in the context of Jacobi's theta functions. We will also discuss briefly possible generalizations of the phenomenon to other systems.

0305-4470/97/090277+07$19.50

Any initial wavefunction $\Psi_0(x)$ in the box extending from $x = 0$ to $x = L$ may be expanded in the basis of eigenfunctions

$$\phi_n(x) = \sqrt{\frac{2}{L}} \sin\left(\frac{n\pi}{L}x\right) \tag{1}$$

with coefficients

$$a_n = \int_0^L \mathrm{d}x\, \phi_n(x)\Psi_0(x). \tag{2}$$

The corresponding eigenenergies

$$E_n = n^2 \frac{1}{2m}\left(\frac{\hbar\pi}{L}\right)^2 = n^2\hbar\frac{2\pi}{T} \tag{3}$$

with $n = 1, 2, 3, \ldots$ determine the so-called revival time $T = 4mL^2/(\pi\hbar)$ of the wavepacket in the box [7].

To keep the argument transparent we now discuss an initial wavefunction Ψ_0 consisting of N equally contributing eigenfunctions, i.e. $a_n = 1$, for $n = 1, \ldots, N$ and $a_n = 0$ for $n > N$. In dimensionless variables $\xi \equiv x/L$ and $\tau \equiv t/T$ for position and time the normalized wavefunction reads

$$\Psi(\xi, \tau) = \sqrt{\frac{2}{N}} \sum_{n=1}^{N} \sin(n\pi\xi) \exp(-2\pi \mathrm{i} n^2 \tau). \tag{4}$$

Figure 1 displays the wavefunctions at $\tau = 0$ made up of 20, 50 and 100 eigenfunctions, respectively. We note that increasing N shifts the centre of the initial state towards the left and leads to sharper localization in position. Figure 2 shows a density plot of the position and time-dependent probability amplitude in the (ξ, τ) plane represented by the absolute value of a wavefunction consisting of 20 eigenfunctions. We observe characteristic rays where $|\Psi(\xi, \tau)|$ assumes low (darkness) and high (brightness) values. These rays emerge either from the left corner ($\xi = 0, \tau = 0$) or from the right corner ($\xi = 1, \tau = 0$) of the spacetime strip. Moreover, there is a characteristic asymmetry between the two types of rays: along the ones from the left corner the wavefunction shows low probability, that is canals. In contrast some of the rays originating from the right corner have high probability, that is ridges. However, canals constantly cut through these ridges creating a chopped structure as seen in the line connecting the upper left corner with the lower right corner in figure 2. We also recognize that additional rays enter the spacetime strip from its sides.

An educated guess for the rays is

$$\xi = l + 2k\tau \tag{5}$$

where l and k are integers. Indeed for $l = 0$ and $k \geqslant 0$, equation (5) describes the rays emerging from the left corner, whereas for $l = 1$ and $k \leqslant 0$ we find the rays whose origin is the right corner. The other values of l such as $l < 0$ and $k > 0$ or $l > 1$ and $k < 0$ give the rays entering the strip at non-zero values of τ.

We gain deeper insight into the functional form equation (5) of these rays when we recall that according to Born [8] the time evolution of a particle with wavefunction Ψ_0 in the box is identical to that of a free particle prepared initially in a periodic array

$$\Psi_{\mathrm{p}}(\xi, \tau = 0) = \sum_{m=-\infty}^{\infty} \Psi_0^-(\xi + 2m) \tag{6}$$

of antisymmetric wavefunctions

$$\Psi_0^-(\xi) \equiv \Psi_0(\xi) - \Psi_0(-\xi). \tag{7}$$

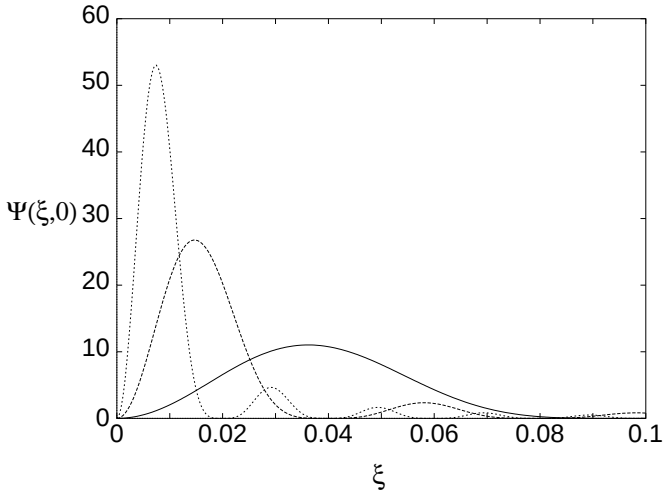

Figure 1. Initial wavefunctions $\Psi_0(\xi, \tau = 0)$ resulting from superpositions of $N = 20$ (full curve), $N = 50$ (long-dash curve) and $N = 100$ (short-dash curve) equally weighted eigenfunctions of the box potential. For increasing number N of contributing eigenstates the initial wavepacket gets narrower and its centre approaches the left wall of the box.

The period of this array is twice the length of the box. Hence in equation (5) even values of $l = 2m$ correspond to the positions of the left wall and its mirror images. In contrast, odd values $l = 2m+1$ represent the positions of the right wall and its mirror images. Therefore, the rays equation (5) are the spacetime trajectories of a free particle starting at time $\tau = 0$ at the right or left wall and their mirror images. Note that according to equation (5) the particle propagates with the dimensionless velocity $v_k \equiv \mathrm{d}\xi/\mathrm{d}\tau = 2k$. Since k is integer, v_k assumes only discrete values. This quantization of velocity is a consequence of the periodicity of the array.

We emphasize that this discussion of the free propagation of the array also throws some light on the difference in behaviour of $\Psi(\xi, \tau)$ along the rays emerging from the two corners $(\xi = 2m, \tau = 0)$ and $(\xi = 2m + 1, \tau = 0)$ corresponding either to the left or the right wall of the box and their mirror images. Indeed these walls are different: whereas the left wall marks the beginning of the periodicity interval of period 2 the right wall is inserted at $\xi = 1$ as to retain from all periodic functions the antisymmetric ones, only. This procedure is necessary since only the latter vanish at the walls at $\xi = 0$ and $\xi = 1$, and hence satisfy the required boundary conditions.

In order to fathom the mathematical reason for the suppression of the wavefunction along some of the rays, equation (5), in the (ξ, τ) plane, we now write the sine function in the wavefunction, equation (4), in terms of exponentials,

$$\Psi(\xi, \tau) = \sqrt{\frac{2}{N}} \frac{1}{2\mathrm{i}} \{\vartheta(\xi, \tau) - \vartheta(-\xi, \tau)\} \tag{8}$$

where we have introduced the finite theta sum

$$\vartheta(\xi, \tau) \equiv \sum_{n=1}^{N} q^{n^2} \, \mathrm{e}^{\mathrm{i}n\pi\xi} \tag{9}$$

with $q \equiv \exp(-2\pi\mathrm{i}\tau)$ [9]. The behaviour of the wavefunction along the rays $\xi = l + 2k\tau$

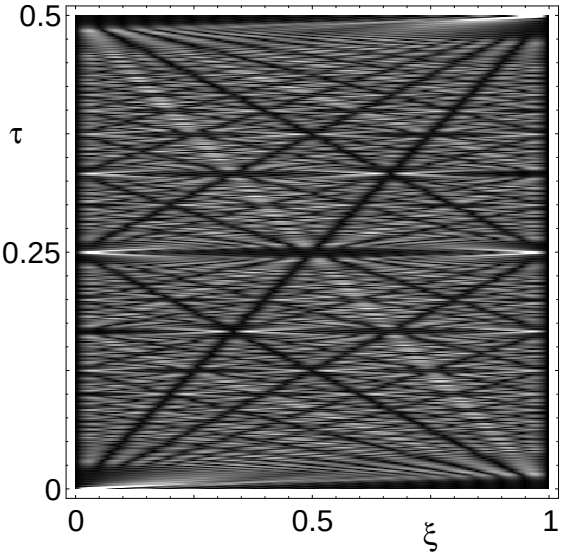

Figure 2. Density plot of the absolute value $|\Psi(\xi,\tau)|$ of a wavefunction in the (ξ,τ) spacetime strip. Darkness displays a low and brightness a high functional value. We note that canals of different steepness emerge from the lower right or left corners of the strip. Moreover, canals enter from the sides. For this example we have considered a wavefunction consisting of 20 eigenfunctions.

follows from

$$\vartheta[\xi = \pm(l + 2k\tau), \tau] = \sum_{n=1}^{N} (-1)^{nl} \exp\{-2\pi \mathrm{i}\tau(n^2 \mp nk)\}. \tag{10}$$

When we complete the square in the exponent we find

$$\vartheta[\xi = \pm(l + 2k\tau), \tau] = q^{-(k/2)^2} \sum_{n=1}^{N} (-1)^{nl} q^{(n\mp k/2)^2} \tag{11}$$

and hence the wavefunction along the rays equation (5) reads

$$\Psi(\xi = l + 2k\tau, \tau) = \sqrt{\frac{2}{N}} \frac{1}{2\mathrm{i}} q^{-(k/2)^2} \sum_{n=1}^{N} (-1)^{nl} [q^{(n-k/2)^2} - q^{(n+k/2)^2}]. \tag{12}$$

We note that each term contributing to this sum is the difference of the two terms $q^{(n-k/2)^2}$ and $q^{(n+k/2)^2}$. Since the powers $(n - k/2)^2$ and $(n + k/2)^2$ are shifted by the number k determining the steepness of the ray, we expect a partial cancellation of these terms provided the number N of terms is much larger than k. Here the prefactor $(-1)^{nl}$ plays a crucial role. Indeed, when l is even this factor is unity and cancellation takes place. However, when l is odd the situation is more complicated. Now cancellation only occurs when k is even. Before we show this we note from equation (12) the symmetry relation

$$\Psi(\xi = l - 2k\tau, \tau) = -\Psi(\xi = l + 2k\tau, \tau) \tag{13}$$

which allows us to confine our discussion to positive values of k only.

We start our analysis of this cancellation effect in equation (12) by introducing the summation index $j \equiv n - k$ in the summation of the first term which yields

$$\Psi(\xi = l + 2k\tau, \tau) = \sqrt{\frac{2}{N}}\frac{1}{2\mathrm{i}}q^{-(k/2)^2}\left\{(-1)^{kl}\sum_{j=1-k}^{N-k}(-1)^{jl}q^{(j+k/2)^2} - \sum_{n=1}^{N}(-1)^{nl}q^{(n+k/2)^2}\right\}. \tag{14}$$

When we recall the relations

$$\sum_{j=1-k}^{N-k} d_j = \sum_{j=1-k}^{0} d_j + \sum_{j=1}^{N-k} d_j = \sum_{n=1}^{k} d_{n-k} + \sum_{j=1}^{N-k} d_j \tag{15}$$

and

$$\sum_{n=1}^{N} d_n = \sum_{n=1}^{N-k} d_n + \sum_{n=N-k+1}^{N} d_n = \sum_{n=1}^{N-k} d_n + \sum_{j=1}^{k} d_{j-k+N} \tag{16}$$

valid for arbitrary coefficients d_j, the wavefunction Ψ along the rays $\xi = l + 2k\tau$ takes the form

$$\Psi(\xi = l + 2k\tau, \tau) = \sqrt{\frac{2}{N}}\frac{1}{2\mathrm{i}}q^{-(k/2)^2}\left\{[(-1)^{kl} - 1]S_{k,l}(N, \tau) + \sum_{n=1}^{k}(-1)^{nl}[q^{(n-k/2)^2} - (-1)^{(N-k)l}q^{(n-k/2+N)^2}]\right\} \tag{17}$$

where

$$S_{k,l}(N, \tau) = \sum_{j=1}^{N-k}(-1)^{jl}\exp[-2\pi\mathrm{i}(j + k/2)^2\tau]. \tag{18}$$

From equation (17) we recognize that for even values of l or k the prefactor of the first sum $S_{k,l}$ vanishes. Moreover, each term of the remaining sum is of the order of unity since $|q| = |\exp(-2\pi\mathrm{i}\tau)| = 1$. Hence we can estimate this sum consisting of k differences of order 2 by $2|k|$. This provides us with the upper bound

$$|\Psi(\xi = 2m + 2k\tau, \tau)| \leqslant \sqrt{\frac{2}{N}}|k| \tag{19}$$

for the absolute value of the wavefunction along the rays $\xi = 2m + 2k\tau$ starting from the left wall and its mirror images. Similarly along the even rays we find $\xi = 2m + 1 + 4k\tau$ emerging from the right wall and its mirror images

$$|\Psi(\xi = 2m + 1 + 4k\tau, \tau)| \leqslant \sqrt{\frac{2}{N}}|2k|. \tag{20}$$

When we confine ourselves to rays of large slope that is small values of $|k|$, that is $|k| \ll N$, we find the inequalities

$$|\Psi(\xi = 2m + 2k\tau, \tau)| \ll 1 \tag{21}$$

and

$$|\Psi(\xi = 2m + 1 + 4k\tau, \tau)| \ll 1. \tag{22}$$

We recall that the modulus $|\Psi(\xi, \tau)|$ of any normalized wavefunction in the box of unit length is unity on average. Hence the inequalities equations (21) and (22) predict that along these rays the modulus $|\Psi|$ falls far below the average value and canals form along these

rays. We also note from equations (19) and (20) that for increasing $|k|$, that is decreasing steepness of the rays, the cancellation of terms in the sum equation (12) becomes less perfect and the canals become less pronounced in complete agreement with figure 2.

Our treatment brings out most clearly that the formation of the canals is indeed a consequence of quantum interference in the wavefunction: the inequalities (21) and (22) follow from the cancellation in (17) which we can trace back to the fact that any wavefunction in the box is a superposition of a right and a left running wave. These waves have a fixed phase difference π, which translates itself into the difference of ϑ sums in equation (8). The difference reflects the fact that the energy eigenfunctions have to satisfy the boundary conditions at the walls. This picture is in complete agreement with [6] which used the Wigner representation to identify these canals as a consequence of the Wigner interference term between the two waves moving against each other.

Let us now briefly discuss the case of odd values of l *and* k when the prefactor of $S_{k,l}$ in equation (17) does not vanish. Hence when we now estimate $|\Psi|$ along these rays we have to take into account the sum $S_{k,l}$. In particular, we have to study its dependence on time τ. Since the sum is similar to the one discussed in the context of curlicues [10] or fractional revivals [5, 11] we can simply borrow the results of these studies. We find† times τ, that is certain rational values of the revival time T for which partial cancellation in $S_{k,l}$ takes place. For these times the wavefunction Ψ falls, as in the case of the canals, far below its average value of unity. However, there also exist times τ where the individual terms in $S_{k,l}$ superpose constructively. In this case the sum $S_{k,l}$, and not the second sum in equation (17), is the dominant contribution to Ψ giving rise to distinct maxima along these rays. From figure 2 we see that indeed every second ray propagating from $(\xi = 1, \tau = 0)$ to the left displays a complicated chopped structure, where for most of the ray a ridge-like behaviour is seen. Again this phenomenon stands out most clearly for steep rays, i.e. small values of k.

Let us mention that this behaviour depends sensitively on the total number of eigenfunctions N. The pattern becomes richer for larger values of N. This fact can be interpreted in the way that an initial state with a large number N of eigenstates resolves the features of the dynamics in the box to a much higher degree than for N small. Our derivation in terms of the eigenfunction expansion directly shows for all cases, l even or odd and k even or odd, that the number of rays $|k|$ which are visible depends on the number of eigenfunctions N contained in the wavefunction. Since the eigenfunctions of a box represent a Fourier basis, by Fourier analysing wavepackets in other potentials one could make use of the methods given here.

We conclude by briefly discussing generalizations of these spacetime structures. According to Born [8] and equations (6) and (7), the boundary conditions of the box impose the antisymmetry of two waves moving against each other. Mimicking this symmetry in a molecular type of potential, Stifter *et al* [6] were able to produce similar effects. Moreover, in another formulation of the probability density in the energy representation, Stifter *et al* [12] have identified the characteristic spacetime lines and have given a relativistic extension. We also recall that the quantum mechanical problem of a particle on a ring can be mapped onto the box problem, if the same boundary conditions are fulfilled. This can be achieved by subtracting opposite angular momentum eigenstates from each other. Let us finally mention that the corresponding problem in classical wave mechanics, i.e. a vibrating string clamped at $\xi = 0$ and $\xi = 1$, shows a much simpler structure in the (ξ, τ) plane because its spectrum is linear in n.

† This also follows from the original wavefunction expansion, equation (4).

In summary we have shown that the spacetime structures in the quantum mechanical probability amplitude for a particle in a square well result from a cancellation in the eigenfunction expansion, equation (4). By using the wavefunction's Jacobi theta function-like properties represented in equation (11) we were able to explain the canals and also the chopped ridges along the rays, (5), in (ξ, τ) space. The details of these spacetime patterns are indeed a property of the wavefunction itself. How much of these details is revealed depends sensitively on the initial wavefunction.

Financial support by the Deutsche Forschungsgemeinschaft through Sonderforschungsbereich 276 and the Gerhard-Hess-Programm, as well as valuable discussions with Gernot Alber, John Briggs, Jens Marklof, Peter Stifter and Alexander Kaplan are gratefully acknowledged.

References

[1] Heller E J 1984 *Phys. Rev. Lett.* **53** 1515
[2] Heller E J and Tomsovic S 1993 *Physics Today* July 38
[3] Alber G and Zoller P 1991 *Phys. Rep.* **199** 231
[4] Kinzel W 1995 *Phys. Bl.* **51** 1190
[5] Berry M V and Klein S 1996 *J. Mod. Opt.* **43** 2139
Berry M V 1996 *J. Phys. A: Math. Gen.* **29** 6617
[6] Stifter P, Leichtle C, Schleich W P and Marklof J 1997 *Z. Naturf.* **52** A 377
[7] Stifter P, Leichtle C, Lamb W E and Schleich W P *Preprint*
[8] Born M 1958 *Z. Phys.* **153** 372
[9] Note that the finite theta sum is closely related to the Jacobi theta functions discussed in: Whittaker E T and Watson G N 1980 *A Course of Modern Analysis* (Cambridge: Cambridge University Press) ch XXI
Hence, we can carry over the methods used there to demonstrate the quasiperiodicity of the theta functions to derive similar relations for ϑ. For a recent review of asymptotic properties of Jacobi theta functions, see also: Marklof J *Proc. IMA Workshop Emerging Applications of Number Theory: Quantum Mechanics (Institute for Mathematics and its Applications, Minneapolis, July 1996)* submitted
[10] Berry M V and Goldberg J 1988 *Nonlinearity* **1** 1
[11] Leichtle C, Averbukh I Sh and Schleich W P 1996 *Phys. Rev. Lett.* **77** 3999
[12] Stifter P, Kaplan A and Schleich W P *Preprint*